

COMPARISON OF BAND RATIOING AND SPECTRAL INDICES METHODS FOR DETECTING ALUNITE AND KAOLINITE MINERALS USING ASTER DATA IN BIGA REGION, TURKEY

B. T. San, E. O. Sumer, B. Gurcay

General Directorate of Mineral Research and Exploration, Remote Sensing Center - 06520, Ankara, TURKEY
tanersan@mta.gov.tr, esumer@mta.gov.tr, boragurcay@mta.gov.tr

KEY WORDS: Remote Sensing, Geology, Comparison, Detection, Multispectral, Method

ABSTRACT:

Advanced Spaceborne Thermal Emission and Reflection Radiometer (ASTER) covers a wide spectral region with 14 bands from visible to the thermal infrared. The different band ranges can be capable of discriminating and mapping surface rocks and predicting pathfinder minerals (i.e. alunite, kaolinite etc.) on alteration assemblages of potential targets. The aim of this study is to compare two different discrimination techniques as band ratioing (BR) and spectral indices (SI) applied on Biga – Çanakkale Area, Turkey. The ground truths were held on 19 locations to compare obtained results. The study area covers altered Miocene age acidic volcanic rocks. Alunite and kaolinite are main minerals in hydrothermal alteration zones. During the image processing, in order to reduce atmospheric effect on ASTER bands, digital numbers of each image channels are converted to relative reflectance for BR and SI techniques. In BR method, two ratios (4/5 and 7/6) were applied to discriminate alunite and kaolinite respectively. However, in SI method, 5 SWIR bands (5, 6, 7, 8, and 9) were taken into account to detect for alunite and kaolinite presence for each mineral. 19 hydrothermal sites were tested by both methods and 13 of them were identified as alunite by using SI method. On the other hand, in BR method, kaolinite and alunite were discriminated in 11 sites and 8 sites, respectively. As a result, SI and BR techniques can detect alunite and kaolinite minerals. SI method gives better results for detecting alunite than that of kaolinite. On the contrary, BR method can be more applicable to discriminate kaolinite than alunite.

1. INTRODUCTION

Advanced Spaceborne Thermal Emission and Reflection Radiometer (ASTER) covers a wide spectral region with 14 bands from visible to the thermal infrared. The different band ranges can be capable of discriminating and mapping surface rocks and predicting pathfinder minerals (i.e. alunite, kaolinite etc.) on alteration assemblages of potential targets (Ninomiya, 2002).

Aim of the study is to compare two different techniques for detection of alunite and kaolinite minerals which are important mineral to illustrate alteration zones.

2. STUDY AREA AND GEOLOGY

Study area, Biga Peninsula, is located on Southern part of the Marmara Sea and North-West part of the Anatolia. It covers a one ASTER scene, size of which has 60 x 60 km area (Figure 1). The study area dominantly consists of volcanic rocks such as andesite, rhyolite type. Most of andesitic rocks were altered by hydrothermal effect. Kaolinite, alunite type minerals and rocks were derived from altered andesite. These kinds of mineral or mineral groups indicate the some metallogenic province such as lead, zinc and copper deposits. Therefore, these alteration minerals are known as indicator minerals for exploration of metallic minerals (MTA-JICA-MMAJ, 1990).

2.1. Geology of Biga Peninsula

The basement of Biga Peninsula consists of pre-Triassic metamorphic rocks are called the Kazdag Group. It is mainly composed of gneiss, amphibolite and marble. This

basement is unconformably overlain by Mesozoic sedimentary formations and Miocene intermediate volcanic rocks. Silicified and argillized alteration zones were identified in some location of the area where volcanism was active during the Eocene to Miocene, and andesite, dacite, rhyolite and pyroclastic rocks are developed. These are widely distributed in the central part of Biga Peninsula (MTA-JICA-MMAJ, 1990). During the beginning of this volcanic period, granodiorite intrusions occurred in many parts. There are three major volcanic activities aged Eocene, Miocene and post-Pliocene. Also, there are two stages of granite activities Triassic and Cretaceous to Eocene. Most of iron, copper, lead and zinc mineralizations are found associated with this type of intrusion. The age of the alteration is inferred to be latest Tertiary, and the center of the Tertiary volcanic activity is very clearly identified (MTA-JICA-MMAJ, 1991.a).

2.2. Mining Activity in the Biga Peninsula

The Biga Peninsula, including the Canakkale Area, is considered to be the most important lead-zinc metallogenic province of Turkey (MTA-JICA-MMAJ, 1991.a). Also, antimony, gold, silver, mercury, iron and other metallic deposits as well as ceramic material resources have been found in the peninsula. Thus, this peninsula has been the target of geological surveys, geochemical prospecting, mining studies and various other projects (MTA-JICA-MMAJ, 1991.b).

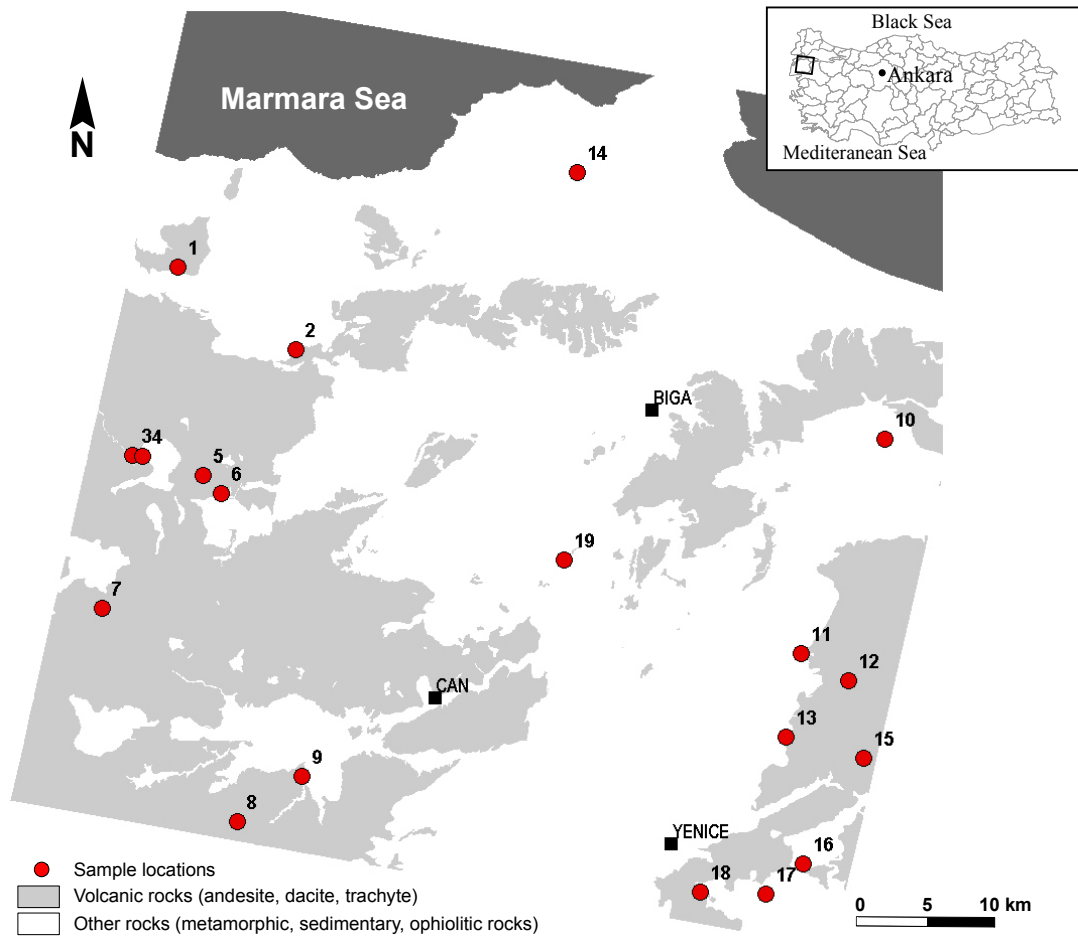


Figure 1. Location of samples on the geological unit map simplified from 1/100 000 scaled geological map

3. METHODOLOGY

During the study, data analyses were carried out using Erdas Imagine and PCI Geomatica image analysis software. In order to find out kaolinite and alunite minerals, two different image processing techniques were performed. These techniques are called as band ratioing and spectral indices techniques (Yamaguchi and Naito, 2003). After applying these techniques, results were compared by using selected sites as ground truth. During the study, an ASTER scene taken at September, 20, 2000 was handled to analyze. Figure 2 summarizes the algorithm which followed during the study.

3.1. Preprocessing

ASTER image has 14 different spectral bands which are 3 VNIR (visible-near infrared), 6 SWIR (short wave infrared) and 5 TIR (thermal infrared) channels (Yamaguchi et al., 1998). Each spectral region has different spatial resolutions such as 15 m (VNIR), 30 m (SWIR) and 90 m (TIR). The most of the image processing methods use same pixel size for all channels due to pixel based arithmetic operations. In order to perform image processes, pixel size of different spectral regions of ASTER image arranged as 15 m cell size for all regions by using PCI Geomatica software. This study

covers only VNIR and SWIR spectral region, TIR spectral region of ASTER did not be used.

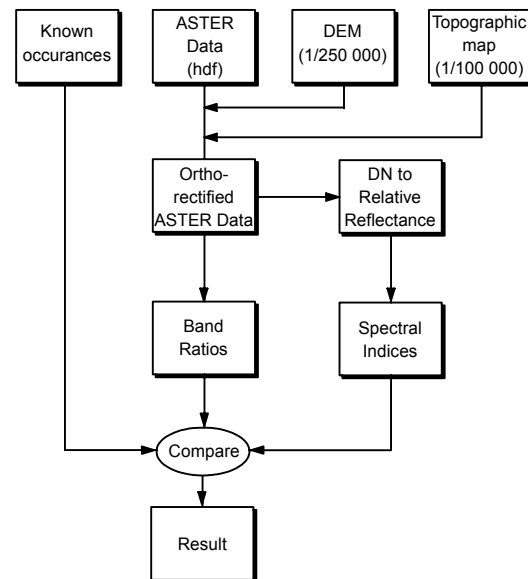


Figure 2. Schematic diagram of the study.

In ASTER data, VNIR and SWIR bands have different spatial resolutions such as 15 m and 30 m respectively. One SWIR pixel covers four VNIR pixels. Because of different pixel size, it is difficult to perform arithmetic operations on pixel base. In order to get rid of this effect, SWIR pixels (30 m) subdivided into four VNIR pixel size (15 m) by using PCI Geomatica software which resulted in more accurate geometric correction with VNIR and SWIR channels in same file. Then, rather than SWIR channels, 15 meter VNIR channels is used for geometric correction.

The next image preprocessing includes the geometric and atmospheric corrections both of which are important to check the results. With the purpose to compare results at the same location, accurate geometric correction should be attained. ASTER scene was geometrically corrected to a UTM (Universal Transverse Mercator) projection using 31 ground control points (GCP) and nearest neighbor resampling technique. During the orthorectification process, 1/100 000 scaled raster topographical map from General Command of Mapping and 1/250 000 scaled DEM (digital elevation model) were used as reference x, y and z data. Finally, ± 0.714 pixel for Easting direction and ± 0.833 pixel for Northing direction residual errors were obtained. Total root mean square (RMS) error was 1.097 pixels for VNIR.

Following these, atmospheric correction should be performed to remove or minimize the effect of atmosphere. There is no need to apply the atmospheric correction for band ratioing in SWIR region. Because SWIR region could not be affected from the atmosphere. The numerator and the denominator in the ratio are nearly affected as the same amount. Nevertheless, it is necessary for spectral indices (SI) method. In order to remove haze effect and convert DN value to relative reflectance value of the image, simple conventional technique which is subtraction of minimum DN value of each band value (Crane, 1971) and division of maximum DN value was used during the study. The minimum DN value of the image can be found in dark pixels from water body such as lake or sea. And also, maximum DN value of the image can be attained in dry salt lake bed rock appearing as bright pixels (Eckhardt and Verdin, 1990). In our study area, there is no any dry lake bed, therefore, maximum DN value was used. Input value of SI method must be reflectance or relative reflectance value. This is because coefficients of the SI method adapted to reflectance value.

3.2. Band Ratioing Method

Each object has its own spectral reflectance pattern in different wavelength portion. Spectral reflectance curve is a kind of fingerprint of the object. The object or rock unit may have high reflectance value in some spectral portion, however, it may absorb in another spectral region. For instance, vegetation has high reflectance in near-infrared (0.78 – 0.86 μm) region and low reflectance in 0.6 – 0.7 μm interval of the spectrum, respectively (Bannari et al., 1995 and Tucker, 1979). According to this information, the main concept of the band ratioing technique was developed for this study. Band ratioing is the very simple and powerful technique in the remote sensing. Basic idea of this technique is to emphasize or

exaggerate the anomaly of the target object (Abrams, 1983).

In our study, alunite and kaolinite minerals are key target to find out any alteration zones. Comparing the spectral reflectance curve of these minerals, 1.6 to 1.7 and 2.145 to 2.185 μm spectral regions are quite important to distinguish alunite minerals from other minerals. Similarly, 2.185 to 2.225 and 2.235 to 2.285 μm spectral regions are important for kaolinite minerals. In 1.6 to 1.7 μm and 2.145 to 2.185 μm spectral intervals are the highest reflectance and absorbance values of the alunite minerals, respectively. On the other hand, 2.235 to 2.285 μm spectral interval is the highest reflectance value of kaolinite minerals and 2.185 to 2.185 μm spectral interval is the lowest reflectance value of the kaolinite minerals (Figure 3). All the corresponding spectral intervals of the ASTER VNIR and SWIR bands can be seen on Table 1.

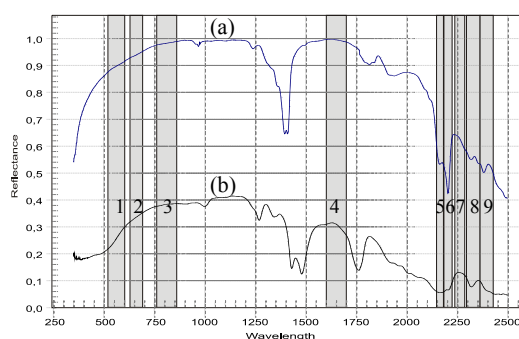


Figure 3. Spectral reflectance curves of kaolinite (a) and alunite (b) minerals within ASTER spectral channels

Alunite and kaolinite minerals have different spectral reflectance pattern. According to spectral reflectance curve of alunite, band 4 (SWIR channel 1) and band 5 (SWIR channel 2) of ASTER data have relatively high and low reflectance, respectively (Figure 3). Then, to emphasize the alunite mineral occurrence, the channel that the alunite has high reflectance is divided into the other channel that of low reflectance. The suitable band ratio for alunite is the ratio of band 4 over band 5. This logic is same as vegetation index calculation. Likewise, high and low reflectance channels are detected as band 7 and band 6 for kaolinite mineral, then ratio of band 7 over band 6 is the proper band ratio (Rowan, and Mars, 2002).

Table 1. ASTER VNIR and SWIR spectral intervals

Subsystem	Band No.	Spectral Range
VNIR	1	0.52 – 0.60
	2	0.63 – 0.69
	3	0.78 – 0.86
SWIR	4	1.6 – 1.7
	5	2.145 – 2.185
	6	2.185 – 2.225
	7	2.235 – 2.285
	8	2.295 – 2.365
	9	2.36 – 2.43

3.3. Spectral Indices Method

Spectral indices method is a kind of orthogonal transformation to be used for surface mineralogical mapping by using the five ASTER SWIR bands (Yamaguchi and Naito, 2003). The spectral indices (SI) method contains mainly five indices, namely, brightness, alunite, kaolinite, calcite and residual indices, respectively.

In general, spectral indices in 6-dimensional (SWIR channels only) spaces can be defined as values measured by projected data points onto imaginary axes with appropriate unit vector directions. Jackson (1983) states that it is kind of orthogonal transformation and the transformed axes are designated to denote specific spectral characteristics. To find out alunite and kaolinite minerals, coefficients of the SWIR bands are obtained in Table 2 (Yamaguchi and Takeda, 2003).

Table 2. Transform Coefficients of spectral indices for the ASTER SWIR bands (Yamaguchi and Takeda, 2003)

Spectral index	Band 5	Band 6	Band 7	Band 8	Band 9
Alunite	-0.511	-0.003	0.802	0.059	-0.304
Kaolinite	0.663	-0.336	0.387	-0.511	-0.191

All SWIR channels were multiplied with their respective special coefficients for alunite and kaolinite minerals, then all calculated SWIR channels were added to obtain indices for those minerals.

4. RESULTS AND DISCUSSIONS

After applying these two methods, the results were checked using existing occurrence data of the study area (Figure 1). According to reference data (occurrence map), 19 hydrothermally altered locations containing both alunite and kaolinite together were compared using existing data and results of two different methods. Resultant imageries have 32-bit DN values, then, to distinguish the minerals from the surrounding pixels or materials, threshold values for each resultant images were computed statistically by using mean value and standard deviations. The 13 of the samples were identified as alunite by using SI method. On the other hand, in BR method, kaolinite and alunite were discriminated in 11 sites and 8 sites, respectively. As a result, SI and BR techniques detected alunite and kaolinite minerals. SI method gives better results for detecting alunite than that of kaolinite. On the contrary, BR method can be more applicable to discriminate kaolinite from alunite.

Table 3 gives the DN value (32-bit) of 19 locations for each method and mean values of the related images. Underlined values in the table are the values above the corresponding threshold level of the each resultant image. The resultant whole image data are normally distributed therefore, threshold level is accepted as mean value of the

related images during the study (Fung and LeDrew, 1988). It is also possible to get optimum threshold value as mean + standard deviation value. However, as the aim is to obtain the lowest threshold value to check the resultant data, mean values are used as the threshold value. Threshold values of the SI method for alunite and kaolinite mineral distinction are 4.034 and 4.54, respectively. According to corresponding threshold values, total 13 samples were clearly discriminated as alunite via SI method. Sample number 3, 6, 13, 14, 17, and 18 have DN values lower than mean value. Therefore, SI method fails on these 6 samples for alunite mineral detection. In addition, SI method could not correctly distinguish kaolinite mineral in selected 19 sites. Using the mean value as threshold level, only 3 samples (sample no: 3, 4, and 10) were correctly detected as kaolinite in this method.

On the other hand, by using band ratio (BR) method 8 samples having the threshold value of 1.304 and 11 samples having threshold value of 0.819 were correctly identified as alunite and kaolinite, respectively. These values are also the mean values of corresponding images of band ratio results.

SI method is more successful for discrimination of the alunite minerals than band ratio method. On the contrary, the results show us that band ratio method is superior to SI method in discriminating kaolinite minerals.

The results could be tested by changing the threshold value. For instance, new threshold value as mean + standard deviation value, 7 and only 1 samples are correctly defined as alunite and kaolinite minerals, respectively. Similar situation also appears in BR method. Correctly detected samples for alunite and kaolinite decrease from 8 to 4 and from 11 to 1, respectively.

5. CONCLUSIONS

In this manuscript, two different approaches are examined to compare for detecting alunite and kaolinite minerals on the study area. One of the techniques is band ratioing method which is performed by division of reflected channel to absorption channel. In our study, optimum ratio for detection of alunite minerals is band 4 over band 5. Furthermore, the optimum band ratio for kaolinite minerals is the division of band 7 to band 6.

Another technique tested in this study is spectral indices method (SI) which is kind of orthogonal projection of SWIR channels. This method is quite successful for detection of alunite minerals. However, it failed in discrimination of kaolinite minerals. During the SI method application, coefficients of the alunite and kaolinite indices are taken from Yamaguchi, Y., and Takeda (2003). Nevertheless, their study was carried out in Nevada, USA. This area almost desert area. Therefore, coefficients of SI should be re-calculated for non-desert or semi-vegetated areas.

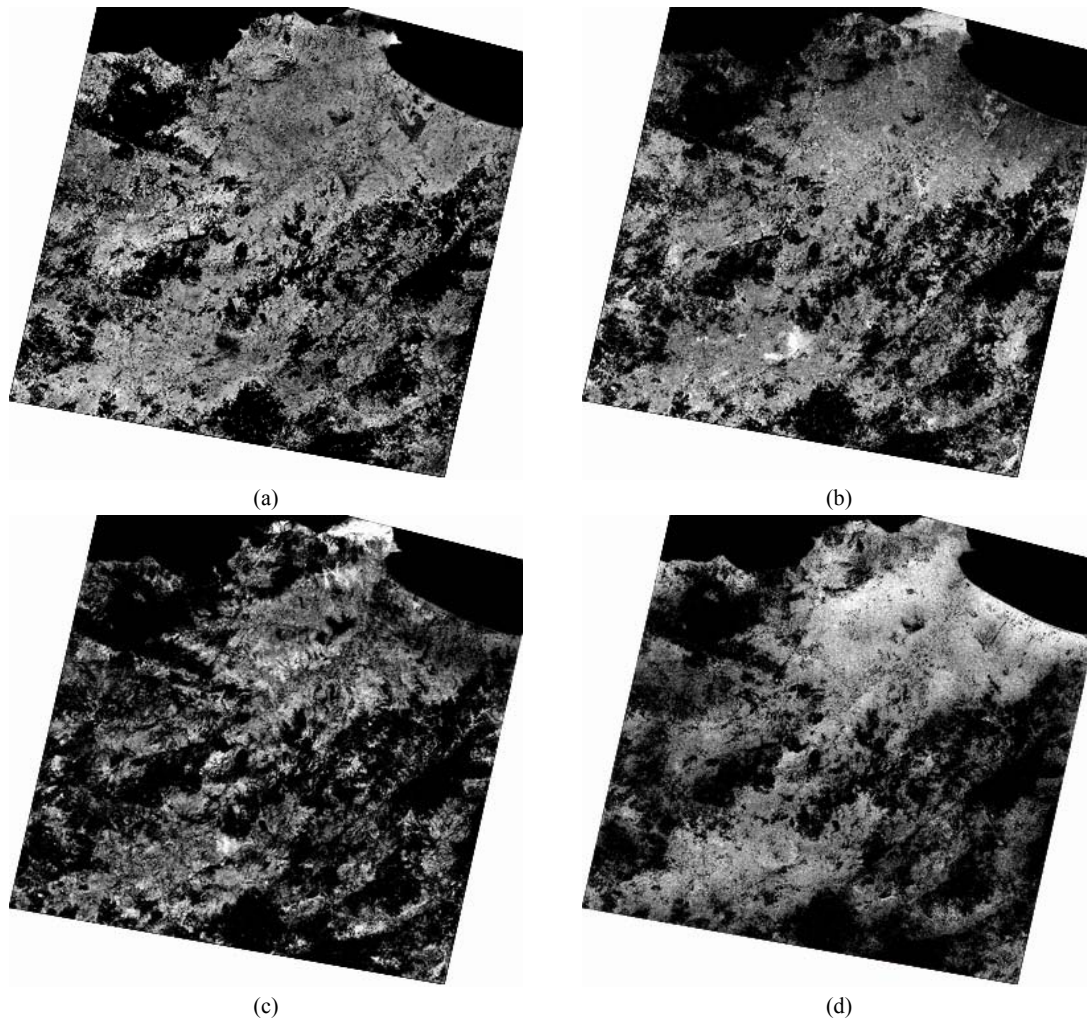


Figure 4. Alunite and kaolinite mineral indices by using band ratioing and SI method. (a) Band ratio results for alunite mineral, (b) Band ratio results for kaolinite mineral, (c) SI method for alunite minerals, and (d) SI method for kaolinite minerals.

Table 3. Checked samples and 32-bit DN value of the samples on the resultant imageries

Sample no.	SI		BR	
	Alunite	Kaolinite	Alunite	Kaolinite
1	<u>4.990</u>	3.665	<u>1.425</u>	0.757
2	<u>6.418</u>	4.059	1.273	<u>0.859</u>
3	3.495	<u>4.954</u>	1.1250	0.780
4	<u>9.434</u>	<u>6.265</u>	1.295	<u>0.900</u>
5	<u>4.797</u>	1.592	1.357	<u>0.907</u>
6	2.949	4.245	1.200	<u>0.841</u>
7	<u>6.540</u>	3.696	1.250	0.805
8	<u>4.742</u>	2.533	<u>1.380</u>	0.783
9	<u>5.050</u>	2.962	<u>1.463</u>	0.753
10	<u>4.677</u>	<u>4.669</u>	<u>1.311</u>	0.782
11	<u>9.687</u>	3.640	<u>1.369</u>	<u>0.911</u>
12	<u>7.717</u>	2.618	<u>1.396</u>	<u>0.894</u>
13	3.405	2.418	<u>1.347</u>	<u>0.879</u>
14	2.022	4.252	1.277	0.712
15	<u>7.827</u>	3.033	1.276	<u>0.908</u>
16	<u>4.991</u>	1.597	<u>1.339</u>	<u>0.889</u>
17	2.159	2.888	1.194	0.724
18	3.600	2.517	1.300	<u>0.827</u>
19	<u>7.600</u>	1.950	1.262	<u>0.928</u>
Total match no. out of 19	13	3	8	11
Mean value of image data	4.034	4.54	1.304	0.819

In practice, band ratio (BR) method is simpler than the SI method. Because, the most of the time, there is no need to apply atmospheric correction in BR. However, only two channels that are reflected and absorbed channels are taken into account in the BR method. On the contrary, five SWIR channels are used to obtain spectral indices in SI method. Logically, using five channel should give more reliable results than the other that of two channels. This study show that SI method could be more suitable for detection of alunite minerals than that of BR method.

6. ACKNOWLEDGMENTS

The authors would like to thank Prof. Dr. Yasushi Yamaguchi (Dept. of Earth and Planetary Sciences, Nagoya University-Nagoya/Japan) for discussion on his developed spectral indices method, and Assist. Prof. Dr. Lutfi Suzen and Assist. Prof. Dr. Nurettin Kaymakci (RS-GIS Lab. Dept. of Geol. Eng., METU-Ankara/Turkey) for their comments. The authors also would like to express their sincere gratitude to Murat Koruyucu (Remote Sensing Center, MTA- Ankara) for his suggestions and evaluations of this manuscript.

7. REFERENCES

- Abrams, J.M., 1983, Remote sensing for porphyry copper deposits in Southern Arizona. *Economic Geology*, 78, pp. 591-604.
- Bannari, A., Morin, D., Bonn, F. and Huete, A.R., 1995, A Review of Vegetation Indices. *Remote Sensing Reviews*, 13, pp. 95-120.
- Crane, R. B. 1971. Preprocessing Techniques to Reduce Atmospheric and Sensor Variability in Multispectral Scanner Data. *Proceedings of the 7th International Symposium on Remote Sensing of Environment*. Ann Arbor, Michigan, p. 1345.
- Eckhardt, D.W. and Verdin, J.P., 1990. Automated update of an irrigated lands GIS using SPOT HRV imagery, *Photogrammetric Engineering and Remote Sensing*, 56(11), pp. 1515-1522.
- Fung, T. and LeDrew, E., 1988. The determination of optimal threshold levels for change detection using various accuracy indices, *Photogrammetric Engineering and Remote Sensing*, 54(10), pp.1449-1454.
- Jackson, R.D, 1983. Spectral indices in n-space. *Remote Sensing of Environment*, 13, pp. 409-421.
- MTA-JICA-MMAJ, 1990, Report on the mineral exploration in the Çanakkale area republic of Turkey, Phase II, *MTA Report*, No: 9000, p. 323.
- MTA-JICA-MMAJ, 1991.a, Report on the mineral exploration in the Çanakkale area republic of Turkey, Consolidated Report, *MTA Report*, No: 9392, p. 180.
- MTA-JICA-MMAJ, 1991.b., Report on the mineral exploration in the Çanakkale area republic of Turkey Phase III, *MTA Report*, No: 9391, p. 229.
- Ninomiya, Y., 2002. Mapping quartz, carbonate minerals and mafic-ultramafic rocks using remotely sensed multispectral thermal infrared ASTER data. *Proceedings of SPIE*, 4710, pp. 191-202.
- Rowan, L. and Mars, J., 2002. Lithological mapping in the Mountain Pass, California area using Advanced Spaceborne Thermal Emission and Reflection Radiometer (ASTER) data. *Remote Sensing of Environment*, 84, pp. 350-366.
- Tucker, C.J., 1979, Red and Photographic Infrared Linear Combinations for Monitoring Vegetation. *Remote Sensing of Environment*, 8, pp. 127-150.
- Yamaguchi, Y., Kahle, A.B., Tsu, H., Kawakami, T., and Pniel, M., 1998. Overview of Advanced Spaceborne Thermal Emission and Reflection Radiometer (ASTER). *IEEE Transactions On Geoscience And Remote Sensing*, 36(4), pp. 1062-1071.
- Yamaguchi, Y., and Naito, C., 2003. Spectral indices for lithologic discrimination and mapping by using the ASTER SWIR bands. *Int. J. Remote Sensing*, 24(22), pp. 4311-4323.
- Yamaguchi, Y., and Takeda, I., 2003. Mineralogical mapping by ASTER in Cuprite, Nevada, USA. *Asian Journal of Geoinformatics*, 3(3), pp. 17-24.